Journal of
Marine Science and Engineering

MDPI

Article

Towards the Development of an Operational Forecast System for the Florida Coast

Vladimir A. Paramygin, Y. Peter Sheng * and Justin R. Davis

Coastal and Oceanographic Engineering Program, University of Florida, Gainesville, FL 32611-6580, USA; pva@coastal.ufl.edu (V.A.P.); justin.r.davis@essie.ufl.edu (J.R.D.)
* Correspondence: pete@coastal.ufl.edu; Tel.: +1-352-294-7764

Academic Editor: Richard P. Signell
Received: 18 July 2016; Accepted: 5 January 2017; Published: 13 January 2017

Abstract: A nowcasting and forecasting system for storm surge, inundation, waves, and baroclinic flow for the Florida coast has been developed. The system is based on dynamically coupled CH3D and SWAN models and can use a variety of modules to provide different input forcing, boundary and initial conditions. The system is completely automated and operates unattended at pre-scheduled intervals as well as in event-triggered mode in response to Atlantic-basin tropical cyclone advisories issued by the National Hurricane Center. The system provides up to 72-h forecasts forward depending on the input dataset duration. Spatially, the system spans the entire Florida coastline by employing four high-resolution domains with resolutions as fine as 10–30 m in the near-shore and overland to allow the system to resolve fine estuarine details such as in the Intracoastal Waterway and minor tributaries. The system has been validated in both hindcast and nowcast/forecast modes using water level and salinity data from a variety of sources and has been found to run robustly during the test periods. Low level products (e.g., raw output datasets) are disseminated using THREDDS while a custom defined web-based graphical user interface (GUI) was developed for high level access.

Keywords: forecasting; storm surge; baroclinic; Florida

1. Introduction

Coastal zones in the U.S. and throughout the world are subject to increasing hazards including storms and storm surge, sea level rise, and harmful algal bloom. Tropical cyclones and associated surge and inundation along the southeastern US coastline area major concern for coastal communities and their economies. Coastal waters in the southeastern US support ecologically and economically significant ecosystems, providing tourism, boating, fishing, and other recreational opportunities with an annual economic benefit of $675+ billion. With 73.5% of the population living in the coastal zone and 77.1% of GDP coming from shore-adjacent counties, this concern about tropical cyclones is particularly important to the State of Florida as it ranks in the top five of US states in the total ocean economy for its reliance on coastal tourism, recreation, and transportation sectors for employment [1,2]. Florida's battle with tropical cyclones is notorious as it has been affected by more hurricanes than any other state. For example, between 1900 and 2010, Monroe County, located along the southwest Florida coast was affected by 32 hurricanes, which is more than any other county in the United States [3].

Management of the Floridian coastal environment is a challenging task for several state and local agencies including Florida Department of Environment Protection, Florida Division of Emergency Management, Water Management Districts, and coastal counties as well as local governments. The work of these agencies is heavily dependent on information made available by such federal agencies as National Oceanic and Atmospheric Administration (NOAA), Federal Emergency Management Agency (FEMA), U. S. Geological Survey (USGS), etc. Within NOAA (the primary agency associated with surge and inundation hazards), the National Weather Service (NWS), National Ocean Service (NOS),

as well as the U.S. Integrated Ocean Observing System (IOOS) provide a multitude of data on the national scale. However, data at physical scales relevant to regional and sub-regional management can be scarce, which makes coastal zone management difficult.

There are several operational and/or quasi-operational forecasting systems for the Florida coast. The National Hurricane Center (NHC) provides the official tropical cyclone surge forecasts, based on the SLOSH [4] and ADCIRC [5] model forecasts. These forecasts provide information for emergency operations and evacuation along the U.S. Atlantic and Gulf coasts. However, both SLOSH and ADCIRC forecasts are based on two-dimensional barotropic models. SLOSH is further constrained in that it uses a coarse grid resolution (on the order of a kilometer) and lacks such important processes as tides, waves, and nonlinear inertia. The Center for Ocean Atmospheric Prediction Studies (COAPS) of Florida State University operates a HYCOM-based 3D forecasting system [6] which possesses robust physics (such as atmospheric-ocean interaction) and 3D baroclinic ocean processes. However, the HYCOM forecasting system uses a relatively coarse grid (>500 m) which is inadequate to resolve the complex coastal and estuarine processes. Similar issues can be found in other Florida forecasting systems based on implementations of the ROMS model [7] and the NCOM model [8] which use relatively course grid resolutions along the Florida coast.

To address the need for a high-resolution forecasting system which can simulate water levels, waves, salinity, and baroclinic circulation along the Florida coast the Advanced Coastal Modeling System (ACMS) was developed. This system can provide forecast information which could be used by the state and local agencies to enhance management of coastal ecosystems and coastal communities in the state of Florida.

Example applications of ACMS forecast information include improved protection of coastal communities from coastal inundation; improved coastal and marine planning and decision-making; improved public health advisories; improved storm surge and rip current warnings; safer and more efficient marine operations and emergency response; advanced decision-making regarding commercial, recreational fisheries and shoreline erosion; improved planning to enhance climate resiliency; improved operational management of water control structures and utility infrastructure by Water Management Districts and utility companies, respectively; and improved emergency operations and management during tropical cyclones via information provided to Weather Forecasting Offices (WFOs) and National Estuarine Research Reserves.

The ACMS is based on the dynamically-coupled CH3D [9–13] and SWAN [14] models which account for wave effects (such as wave-induced wind stresses, wave-current interaction which includes radiation stresses throughout the water column and wave-current bottom stresses) and can incorporate a variety of input forcing functions and boundary and initial conditions for driving these models. The system is automated and can be run at pre-scheduled intervals or be triggered by such events as tropical storm advisories by the National Hurricane Center.

Another significant issue to be considered for operational modeling is computational efficiency. Multiple (often over ten) forecasting model runs with high grid resolutions every day require significant computing resources. A forecasting system must be able to produce timely forecasts, since the value of forecast products declines quickly with the time it takes to produce them.

In the remainder of this paper, ACMS is first described, followed by a description of the model setup, and example model validations.

2. Materials and Methods

2.1. The ACMS Modeling System

2.1.1. CH3D

CH3D (Curvilinear Hydrodynamics in 3D) is a hydrodynamic model originally developed by Sheng [9,10]. The model can simulate 2-D and 3-D barotropic and baroclinic circulation driven by tide, wind, density gradients, and waves. CH3D uses a boundary-fitted non-orthogonal curvilinear grid

in the horizontal direction and a terrain-following sigma grid in the vertical direction. As such, the model can accurately represent complex shoreline and geometries in coastal regions. It uses a robust turbulence closure model to represent vertical turbulent mixing [15] and a Smagorinsky type model for horizontal turbulent mixing. The model uses bathymetry and topography which are referenced to the NAVD88 vertical datum for all domains to accurately simulate the coastal inundation. CH3D has been applied to such water bodies as Charlotte Harbor, Biscayne Bay, Apalachicola Bay, Florida Bay, Indian River Lagoon, Lake Okeechobee, Lake Apopka, Sarasota Bay, St. Johns River, Tampa Bay, Naples Bay, and Rookery Bay in Florida, as well as Chesapeake Bay, New York Bight, Long Island Sound, and the Gulf of Mexico.

2.1.2. CH3D-IMS

CH3D has been coupled to models of wave, sediment transport, water quality, light attenuation, and sea grass dynamics to produce CH3D-IMS [16], an Integrated Modeling System for simulating the response of estuarine and coastal ecosystems to anthropogenic (e.g., increased nutrient loading) and natural (e.g., sea level rise) changes.

2.1.3. CH3D-SSMS

CH3D-SSMS (Storm Surge Modeling System) is a modeling suite that features coupled CH3D and SWAN models for coastal dynamics and large scale surge-wave models that are used to extract boundary conditions for the coastal model [11,17], which has been used extensively to simulate storm surge and inundation due to various tropical cyclones including Hurricanes Charley (2004), Dennis (2005), Isabel (2003), Frances (2004), Ivan (2004), Jeanne (2004), Katrina (2005), Wilma (2005), Katrina (2005), Ike (2009), Sandy (2012), Matthew (2016), and others [11–13,17–19]. Details of the CH3D model, including equations of motion and boundary and initial conditions, are described in [11]. CH3D-SSMS contains a robust flooding and drying scheme which is an extension of that developed by Davis and Sheng [20].

In a regional storm surge and coastal inundation model Testbed [21], CH3D-SSMS was compared with ADCIRC [5], CMEPS [22], FVCOM [23], and SLOSH [4]. Detailed comparisons of models were made in terms of simulated storm surges during historic storms as well as coastal inundation maps including the surge atlas and the 1% annual chance coastal inundation maps which is also known as the Base Flood Elevation (BFE) according to the Federal Emergency Management Agency (FEMA) of the US [24]. The results of CH3D-SSMS were found to compare well with observed water level data and was as accurate as other models. The computational efficiency of CH3D-SSMS is only inferior to the extremely efficient SLOSH model which uses a very coarse grid (~1 km) and has simpler physics. The model Testbed results demonstrated that, to obtain accurate model results efficiently, it is feasible to use a highly efficient coastal surge-wave model, e.g., CH3D-SWAN, with high resolution in the coastal region, and couple it to large-scale surge-wave models with coarser resolution in the offshore region. Alternatively, one can use an unstructured grid surge-wave model for the coastal and offshore domains with a single grid, but a high-resolution grid in the coastal region often results in stringent computational time step limitation and requires dramatically more computational resources.

CH3D suites continue to be improved as new research enables incorporation of more dynamic features, e.g., vegetation effects on storm surge, into the models. For example, Lapetina and Sheng [25] recently used the vegetation-resolving ACMS to simulate the effects of vegetation, three-dimensionality, and onshore sediment transport on complex storm surge dynamics during Hurricane Ike which inflicted major damage to the Texas coast in 2009. Results of the 3D model are found to be more accurate than 2D model results.

2.2. ACMS

The cornerstone of the ACMS modeling system includes the CH3D (shallow water hydrodynamics) and SWAN (wave) models, running on four domains (Figure 1) that span the entire Florida coast.

The two models are dynamically coupled, which enables representation of complex physics such as vertically varying wave-current interaction. ACMS is essentially the integration of CH3D-SSMS and CH3D-IMS which was described in the previous section.

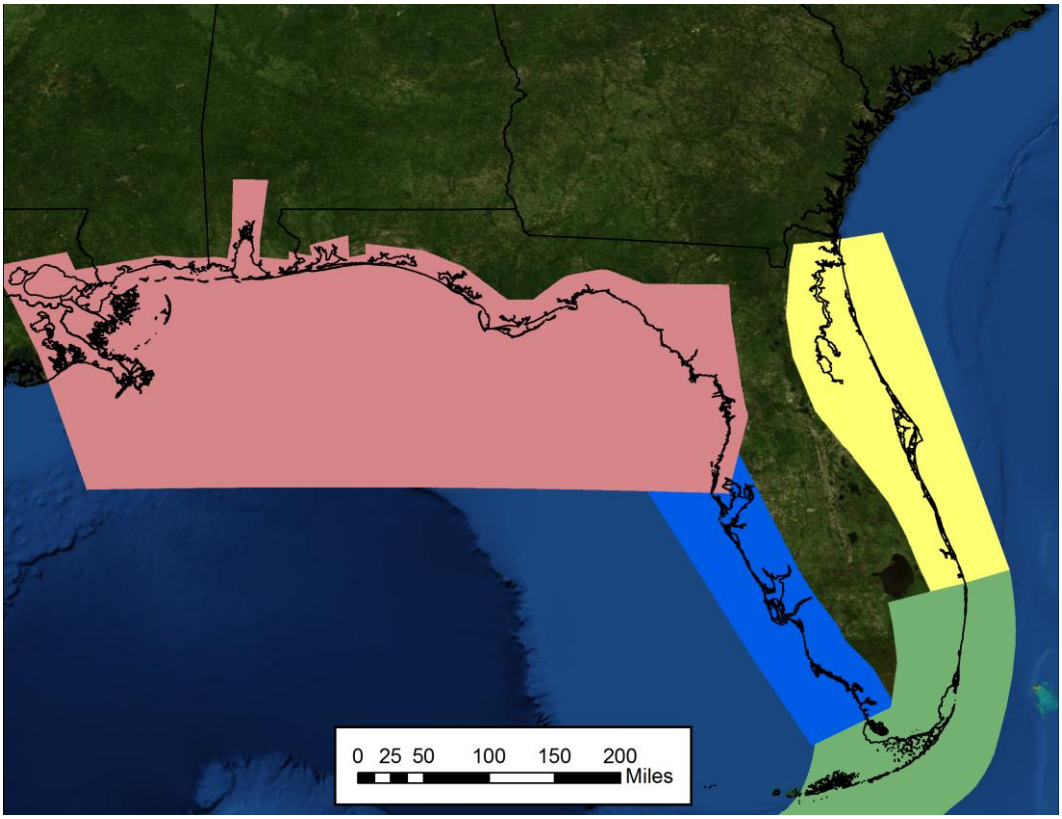

Figure 1. Advanced Coastal Modeling System (ACMS) Florida coast domains: Northern Gulf (NG) of Mexico (pink), Southwest (SW) (blue), Southeast (SE) (green), and East Coast (EC) (yellow).

SWAN is a third-generation phase-averaged wave model that can be applied to nearshore wave modeling. The model can use a variety of computational grid arrangements including non-orthogonal regular, curvilinear, and unstructured triangular grids. SWAN accounts for wave propagation in time and space, shoaling, refraction due to currents and depth, frequency shifting due to currents and dynamic depth, wave generation by wind, energy dissipation by bottom friction, depth-induced breaking and transmission through and reflection from obstacles (full or partial reflection can be considered). SWAN represents waves using a two-dimensional wave action density energy spectrum and the evolution of the spectrum is described by the spectral action balance equation in which a local rate of change of action density in time is related to the propagation of action in geographical space, shifting of relative frequency due to currents and depths, depth-induced and current-induced refraction balanced by the source term in terms of energy density representing the effects of energy generation, energy dissipation and nonlinear wave-wave interactions.

ACMS can use a variety of wind fields such as

- Hurricane Research Division's H*Wind [26];
- Navy's NOGAPS [27];
- GFDL [28];
- NAM (North American Mesoscale) that uses WRF (Weather Research and Forecasting model [29]) and is run by the National Centers for Environmental Prediction [30]; and

- Several synthetic parametric wind models driven by storm parameters that are derived from National Hurricane Center (NHC) predictions.

2.3. ACMS Modules and Workflow

ACMS consists of four main modules (Figure 2): (1) data acquisition and pre-processing module; (2) simulation setup (staging/running/etc.) and job management module; (3) post-processing module; and (4) visualization module. These modules provide automation of such processes as input data acquisition, archiving and cataloging of data and model results, data pre-processing, setting up model simulations, running and monitoring jobs, post-processing of model results, and visualization. Some of the most important properties of the ACMS are full automation, compliance with existing standards for ocean data, and efficient use of available computational resources. Previous implementation of the system showed that it can perform both 3D baroclinic and storm surge simulations simultaneously during tropical cyclones [18], as well as ensemble forecasting of storm surges based on an ensemble of storm tracks generated from the probability distribution of previous track forecasting errors [31].

The data acquisition module is responsible for data acquisition and consists of monitors that poll the data providers for new data and acquires the data as it becomes available. Monitors for a variety of datasets are available: NOAA NHC advisories, the U.S. Navy's Automated Tropical Cyclone Forecasting System (ATCF [32]) forecast products, atmospheric inputs (NAM, NOGAPS, GFDL, etc.), boundary and initial conditions for circulation from such models as HYCOM [33] and ROMS, and boundary and initial conditions for waves from wave models such as WaveWatch III (WWIII) [34]. River flow measurements and predictions, salinity measurements, etc. are also collected where available from USGS, National Estuarine Research Reserves, and the National Weather Service River Forecast Center. All the data are obtained as they become available, processed (with QA/QC, subsetting, and necessary format conversions), archived, and cataloged (using a MySQL database).

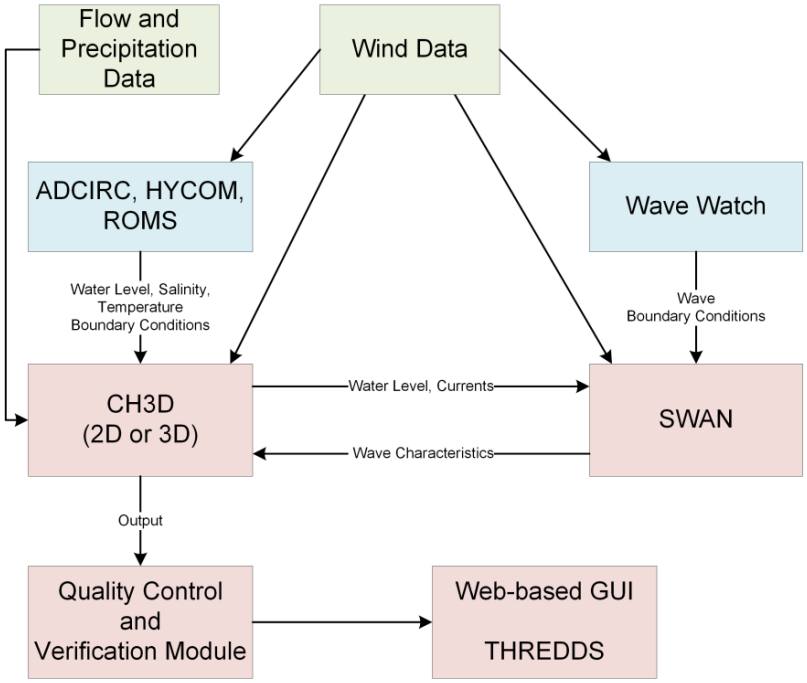

Figure 2. ACMS workflow diagram.

ACMS supports two modes of operation:

- Event triggered, where a model instance is created as a response to an event (such as an NHC-issued tropical cyclone advisory) or

- Preset cycles, where a model is initiated at fixed times, which usually follow the standard 4-cycles per day scheme (model initialized at 00:00, 06:00, 12:00 and 18:00 UTC).

The job management module initiates the simulation and polls the data acquisition module. Once all the data necessary for model input is collected, the module generates the necessary input files, sends the job to the computing cluster via HTCondor job management system [35] and monitors the job status for potential computing resource failures in which case the jobs are resubmitted to alternate resources.

The post-processing module extracts output from completed forecast runs, generates aggregate products, calculates statistics, and places products and outputs in the archive. ACMS currently uses NetCDF with CF-1.5 conventions as a data format of choice and Unidata's THREDDS Data Server [36] as the main platform for data distribution. Visualization module (mostly client-based) is written in JavaScript and uses THREDDS server (via WMS feeds and NetCDF subsetting) as a data provider to display data in a user-friendly manner (Figure 3).

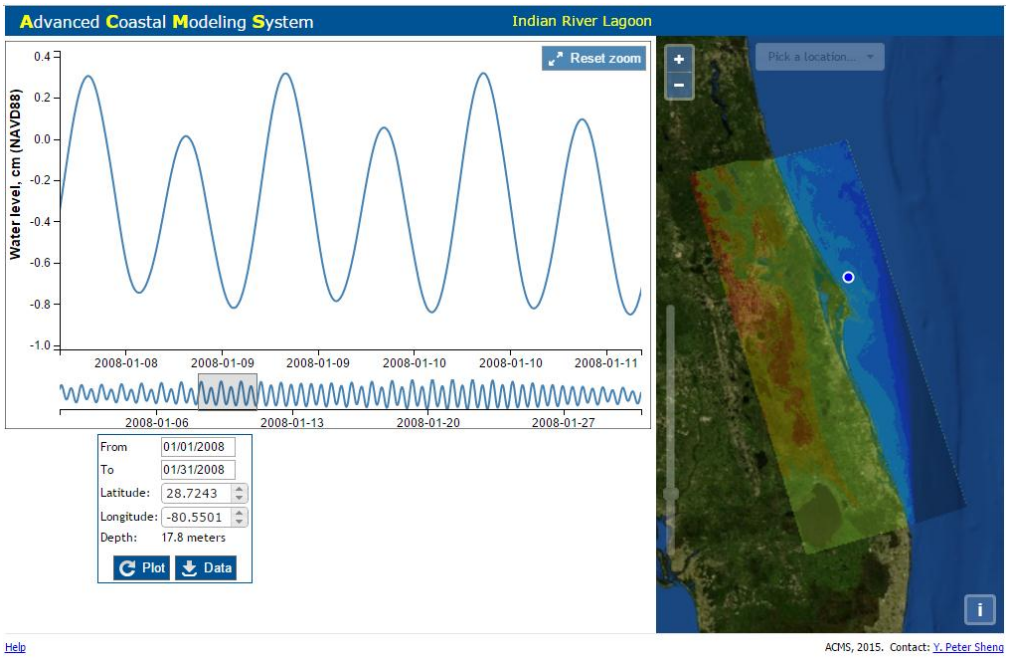

Figure 3. Sample ACMS web-based interface for data preview and download developed for St. Johns River Water Management District with focus on the Indian River Lagoon on the east coast of Florida.

Data availability is the limiting factor for initiating a new forecast cycle. A complete data set such as wind, the waves at the open boundary, the surge at the open boundary, and the flow rates at rivers should be available from the archive for the forecast cycle to be initiated. Data is pulled from the archive by the Data Processing Module and all necessary input files are generated for all the simulations that are scheduled to run within that cycle. Completion of this process triggers the start of the cycle at the Core Module which is responsible for setting up the boundary conditions for all the models involved in the cycle, scheduling, and submitting the simulation to one of the available computational resources. There are mechanisms that enable forecasts even when some of the data is missing. Certain data such as missing atmospheric snapshots or relatively short gaps in time-series data can be reconstructed, interpolated or extrapolated based on available data.

2.4. ACMS Model Setup

Two implementations of ACMS are discussed in this paper:

1. 2D implementation—The 2D barotropic CH3D model is coupled with SWAN and CH3D receives open boundary conditions from a large-scale ADCIRC model running on a coarse grid ~2–5 km, while SWAN receives open boundary condition from WWIII. Despite the coarseness of the grid, ADCIRC produces satisfactory results along the offshore CH3D boundary and runs very quickly to allow syncing with the CH3D model. This implementation is event-triggered by NHC tropical cyclone advisories. ACMS downloads NHC advisories and, whenever it contains forecasted tropical cyclone track coming within 100 miles of a CH3D domain, creates a model instance for that advisory. This implementation is used to quickly forecast storm surge and inundation during tropical storms. Not only do 2D model simulations complete quicker, but all the inputs required for the model are also contained in the advisory, because the surge and wave models are driven by a synthetic parametric model for atmospheric wind and pressure. In most cases, the amount of time between the advisory time stamp and prediction is less than two hours.
2. 3D Implementation—The 3D baroclinic CH3D model is coupled with SWAN, and CH3D receives boundary conditions from a large-scale HYCOM or ROMS model, while SWAN receives open boundary condition from WWIII. The model runs four times a day at 6-h intervals starting at 00:00 UTC. This implementation is intended to provide more comprehensive forecasts including water levels, waves, baroclinic circulation, and salinity. However, this increased fidelity comes at a cost: not only the model runtime increases to 4–6 h (depending on domain and conditions such as networking and transfer speeds, etc.), but the time required to fetch all the inputs (including open boundary conditions from HYCOM or ROMS, atmospheric predictions from NAM, and river flows, etc.) can be twice as long. The model has the capability to simulate temperature, however, due to limited data available for boundary conditions and verification, current forecasting implementation does not include temperature simulation.

2.4.1. Atmospheric Forcing

Atmospheric forcing in ACMS includes atmospheric pressure, wind, and precipitation. The system can use a variety of wind fields as well as several synthetic parametric models. The 2D implementation uses the parametric model of Xie et al. [37]. Model parameters such as location of the storm, maximum wind, and radii to 34 kt, 50 kt, and 64 kt winds are based on the NHC predicted storm parameters. The 3D implementation is driven by the atmospheric forcing predicted by the NAM model.

2.4.2. Surge-Wave Coupling

In ACMS, the CH3D model is dynamically coupled to the SWAN wave model [14]: wave results obtained by SWAN are passed to CH3D and water depths and currents obtained by CH3D are passed onto SWAN. This accounts for wave setup and wave-current interaction within the CH3D model, which features several formulations for calculating wave stresses [38], including vertically varying formulations (e.g., Mellor [39]) as well as the vertically uniform formulation of Longuet-Higgins and Stewart [40,41]. The 3D implementation of the model uses the formulation by Mellor [39] as it was found to produce more accurate results [38].

The time step used for CH3D simulation is 60 s and time step used for SWAN simulation is 5 min, which is when the two models exchange information.

2.4.3. Coastal-Offshore Coupling

Both coastal CH3D and SWAN models use the same non-orthogonal curvilinear model grid and are dependent upon open boundary conditions provided by larger scale ocean models. ACMS interfaces enable it to receive boundary conditions from a variety of large-scale models such as HYCOM, ROMS, CH3D, and ADCIRC for CH3D, and larger-scale SWAN or WWIII for SWAN.

In the 2D implementation, CH3D obtains open boundary conditions (elevation at the open boundary) from a coarse-grid (~2–5 km) ADCIRC model which is run simultaneously with the CH3D model. Large-scale SWAN model produces boundary conditions for the coastal SWAN model.

In the 3D implementation, CH3D obtains open boundary conditions (vertically varying currents and salinity) from a HYCOM, while SWAN derives its boundary conditions either from a WWIII model or a large-scale SWAN model.

2.4.4. ACMS Model Domains and Forecast Cycles

The four domains used by ACMS span the entire Florida coastline (Figure 1) and extend 50–100 km offshore (Table 1). The forecasts range from 48 h up to 72 h, depending on the configuration and available input. Each cycle is initialized from the previous cycle, and a 6-h nowcasting is performed to fill the 6-h gap between cycles, followed by a forecast.

ACMS model domains use NAVD88 as a vertical datum of choice, which makes computing surge, inundation, and flooding a simple and transparent process since all the topography data is generally referenced to NAVD88. The 3D implementation of the model typically uses six equally spaced sigma layers in vertical—this number was determined by comparing simulations obtained with 4, 6, 8, 16 layers, which found that 6 layers were sufficient to resolve the pycnocline and that going from 6 to 8+ layers provides negligible differences in simulation results.

Table 1. Characteristics of Advanced Coastal Modeling System (ACMS) model domains.

Domain	Minimum Resolution (m)	Approximate Grid Cell Count	Average Offshore Extent (km)
East Coast (EC)	32	339,000	55
Southeast (SE)	21	607,000	60
Southwest (SW)	29	366,000	65
Northern Gulf of Mexico (NG)	47	404,000	75

2.4.5. Boundary Conditions

The water level at the open boundary of CH3D domain is prescribed by combining the water level predicted by a regional ocean circulation model and spatially varying tidal constituents which include M2, S2, N2, K2, K1, O1, P1, Q1, SA, and SSA. These tidal constituents were determined to be important for the Florida coast based on the NOAA tidal gauge data, while other constituents generally are estimated to have an amplitude of less than 1 cm. The constituents at the open boundary are developed via an iterative process in which phases and amplitudes at the open boundary are adjusted during tide-only simulations to provide the best possible fit with observed tides at the coastal stations. Salinity at the open ocean boundary is interpolated from a 1/12 degree HYCOM or ROMS (provided at 6-h intervals).

Open boundary conditions for SWAN are wave height and period obtained from the results of a 0.25 degree WWIII model.

River flow measurements/forecasts and salinity measurements are gathered from a variety of sources such as NOAA Advanced Hydrologic Prediction Service, Florida DEP, Florida Water Management Districts, and National Estuarine Research Reserves. These data serve as boundary conditions for flow and salinity upstream of rivers and creeks and are crucial to accurate predictions of currents and salinity in estuaries, inlets, and near-shore zone. River flow and salinity data used for boundary conditions in estuaries are extrapolated in time based on the trend identified in previous data for stations where flow forecasts are unavailable or the forecasted period is shorter than the length of ACMS forecast. The extrapolation is based on identifying a linear trend during the last 7 days and using it to extrapolate the flow (subject to a maximum increase/decrease of 2 ppt in a 7-day period). This was found to produce slightly better results compared to using the last available value for the entire forecast period.

3. Results

3.1. Model Validation

Using the model setup described in the previous section, a series of validation tests were performed by hindcasting non-storm events (lighter wind speeds, tidally-dominated flow) as well as several tropical cyclones including Andrew (1992), Jeanne (2004), Wilma (2005), and Fay (2008). The storms are selected to represent different hurricanes ranging from slow moving Tropical Storm Fay, which became almost stationary for about a day just off the east coast of Florida near Jacksonville, to fast-paced Hurricane Wilma that went across the entire state in less than six hours with significant variation in intensity and size. Some forecast results are also presented since the ACMS system has been running in the quasi-operational mode since 2012. Only a select few stations (Figure 4) per domain are shown here as it would be impossible to show model-data comparisons for all of them in the scope of this paper.

Figure 4. Location of select data stations used for ACMS validation.

3.1.1. Non-Storm Conditions

Simulation of tides is a key feature of a forecasting system because water levels and currents are very important for safe navigation and recreation as well as the increasing coastal inundation during high tides. Under calmer weather conditions, tides usually dominate and determine the coastal circulation. Hence, the ability to accurately predict tidal water level and flows is crucial. Data during 2008–2014 were used for validation purposes and the criterium for tidal validation is to achieve an average RMS error of 7 cm per domain. The total number of stations used for validation of tides is: nine for the EC domain, five for the SE domain, five for the SW and six for the NG domains. Vilano Beach (Figure 5) and Melbourne (Figure 6) stations are examples of tidal simulations on the EC domain.

Data from a NOAA station at Naples, FL (Figure 7) on the west coast was used to validate the tides for the SW domain.

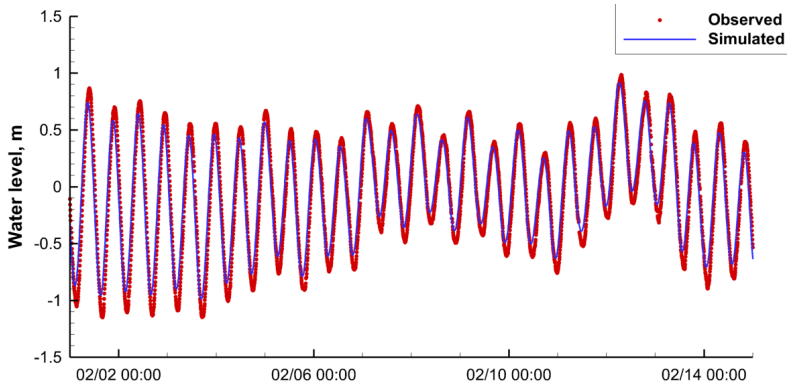

Figure 5. Comparison of simulated (hindcast) and observed water levels at Vilano Beach station for tidally-dominated flow.

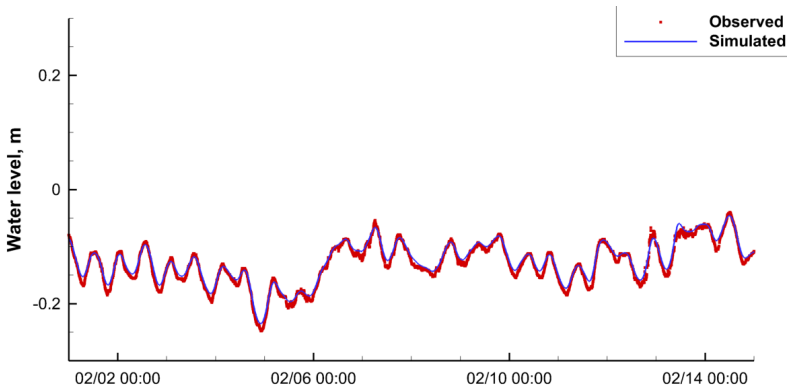

Figure 6. Comparison of simulated (hindcast) and observed water levels at Melbourne station for tidally-dominated flow.

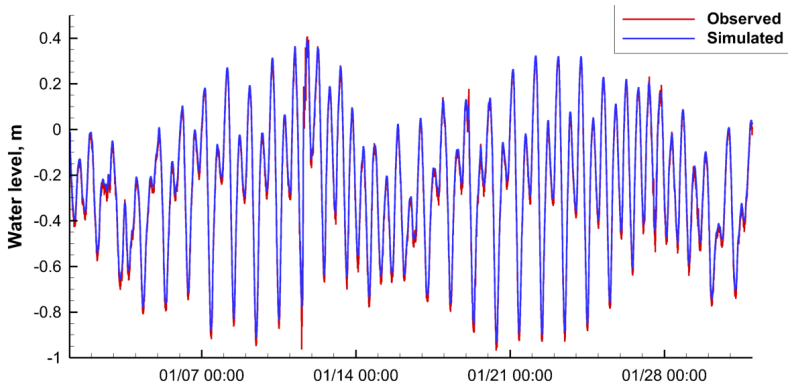

Figure 7. Comparison of simulated (hindcast) and observed water levels at Naples station for tidally-dominated flow.

Tidal Simulation

Overall, ACMS predicted amplitudes and phases of select tidal constituents (M2, S2, N2, K2, K1, O1, P1, Q1, SA, and SSA) are very close to the observed values at all stations with the average RMS error being under 5%.

Nuisance Flooding

The ACMS was used to forecast "king" tides (astronomically high tides) near Miami Beach (Figure 8), and the results were provided to the city of Miami Beach. During a "king" tide, numerous South Florida communities (Miami Beach, Fort Lauderdale, Key West, and Naples, etc.) experience nuisance flooding with streets inundated of 30 cm or more. Nuisance flooding is occurring more frequently as the sea level continues to rise. By 2050 some communities (e.g., Key West) are expected to have nuisance flooding during more than 100 days per year. The City of Miami Beach installed 20 pumps in 2015 to mitigate nuisance flooding during king tides.

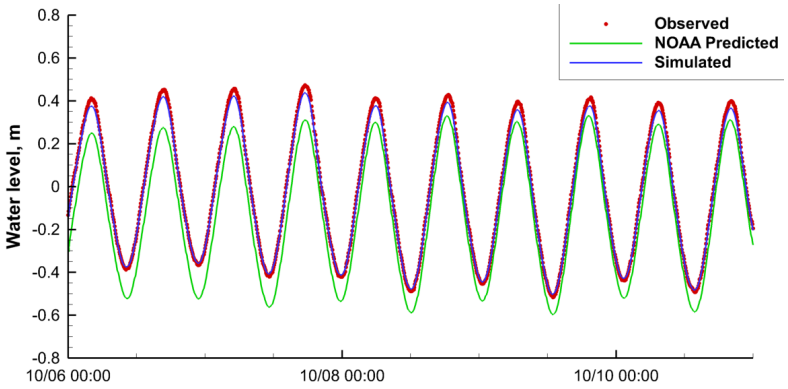

Figure 8. Forecast of "king" tides and comparison with National Oceanic and Atmospheric Administration (NOAA) observed and predicted water levels at Virginia Key station in October 2014 (initialization time: 6 October, 2014 00:00Z).

Salinity Simulation

Limited salinity data was available for validation with just two stations for the EC and SE domains, five stations clustered inside the Naples/Rookery Bay region on the west coast of Florida and a few in the Apalachicola Bay maintained by the Apalachicola National Estuarine Research Reserve (ANERR). The quality of salinity predictions can vary drastically depending on availability and accuracy of river flow predictions. However, most stations show satisfactory agreement. The RMS error in the SW domain during September and October 2014 varied between 2 ppt and 7 ppt with a correlation coefficient (r^2) between 0.52 and 0.9. The NG domain comparisons (Figure 9) show slightly better agreement with the RMS error between 2 ppt and 5 ppt. The RMS errors for stations in the EC domain vary between 3 ppt and 9 ppt, most likely due to the inaccuracy and limited availability of river flow data that provides fresh water inflow into the model domains.

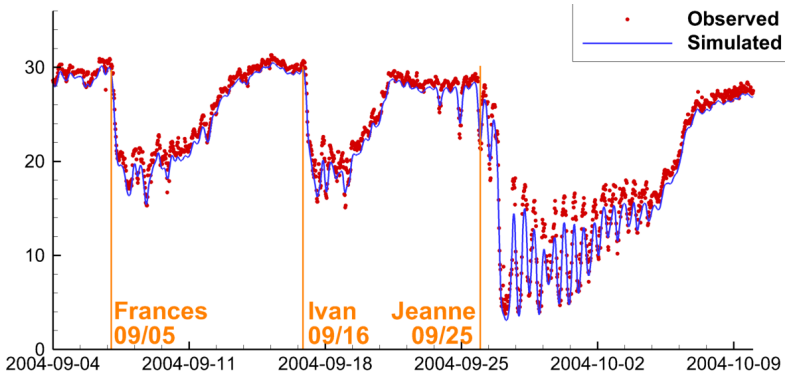

Figure 9. Comparison of simulated and observed salinity Cat Point station (NG domain), orange vertical lines indicate land fall times of the three storms: Frances, Ivan, and Jeanne.

Surface Current Simulation

There exist limited datasets of observed surface currents collected by the high frequency radar (HF Radar, [42,43]) along the southeast coast of Florida near Biscayne Bay. The ACMS simulated currents in the central part of the coastal domain appear to be comparable (Figure 10) with the observed data. However, it should be noted that these currents data have not been fully analyzed to remove errors associated with interference of the radar signals.

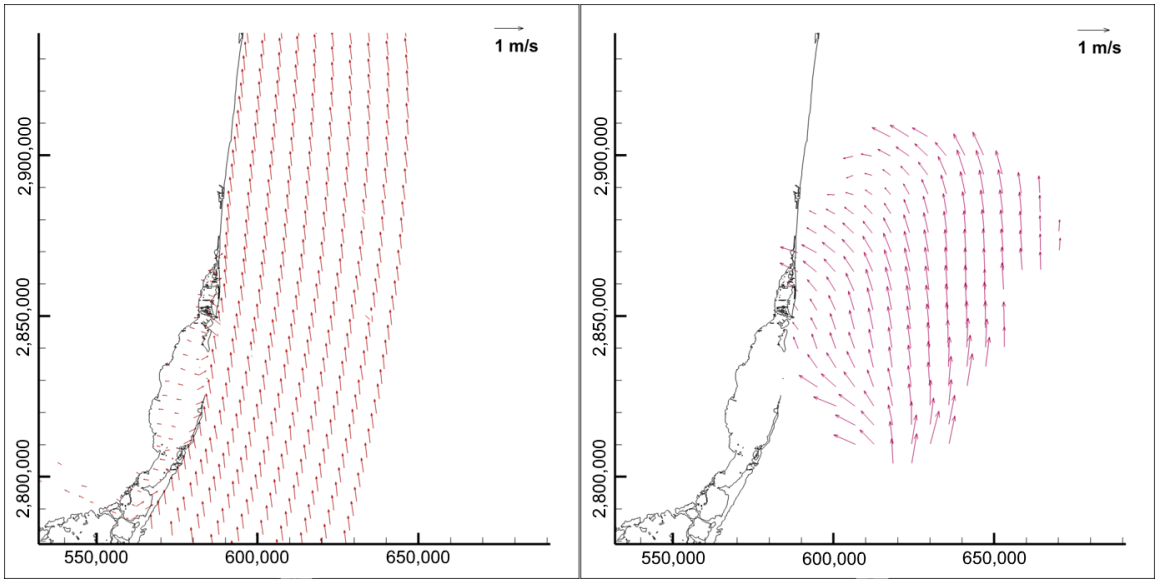

(**a**) (**b**)

Figure 10. Comparison of estimated surface currents (**a**) vs. surface currents measured by the HF Radar (**b**) east of the Biscayne Bay (SE domain, 20 March 2014 12:00Z). Coordinate space is UTM zone 17N (m).

3.1.2. Simulation of Surge, Wave, and Inundation during Tropical Cyclones

Model validations for tropical cyclone conditions were carried out in a hindcast mode for the following four storms: Hurricane Andrew (1992), Hurricane Jeanne (2004), Hurricane Wilma (2005), and Tropical Storm Fay (2008).

Hurricane Andrew

Andrew was a small but ferocious hurricane that brought unprecedented economic devastation to the southern Florida peninsula. Overall damage in the U.S. is estimated at ~$26.5 billion (1993 USD) making it one of the five costliest storms in U.S. history. The tropical cyclone struck southern Dade County, Florida (Figure 11) especially hard, with violent winds and storm surges characteristic of a category 5 hurricane [44] on the Saffir/Simpson Hurricane Scale, and with a central pressure of 922 mb. Unfortunately, the amount of data available for Andrew is limited to a single station at Haulover Pier, but the model predicted water level at this station compared very well with the observed data (Figure 12), especially when the wave model is coupled to the surge model in the simulation.

Figure 11. Track of Hurricane Andrew (1992).

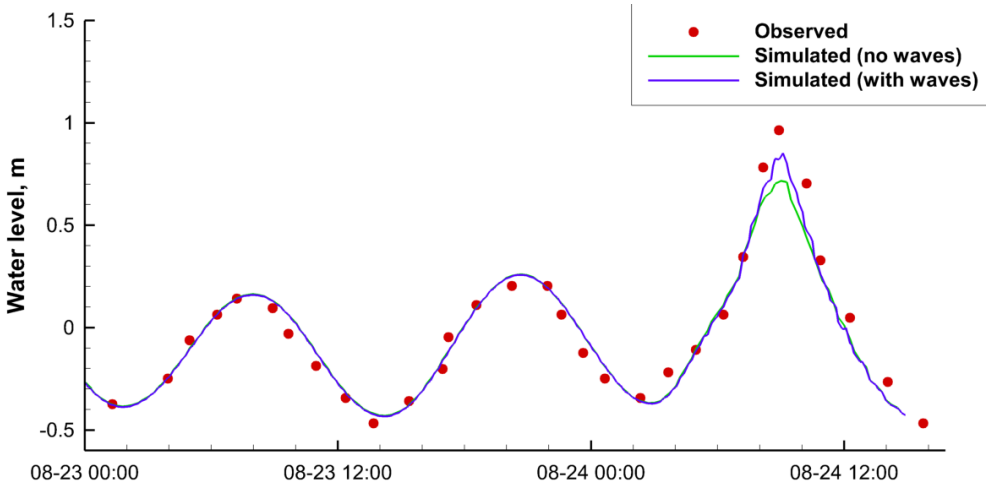

Figure 12. Comparison of observed and simulated (hindcast) water levels at the Haulover Pier station during Hurricane Andrew (1992). "No waves" curve shows results based on CH3D model that does not include wave effects and "with waves" shows results based on the coupled CH3D-SWAN model.

Hurricane Jeanne

Hurricane Jeanne (Figure 13), while known as a very deadly storm claiming more than 3000 lives in Haiti alone, weakened significantly before making its landfall on the east coast of Florida near Stuart [45]. After which, it further weakened to a tropical cyclone making its way across Florida peninsula towards Tampa. Because of its smaller size (about 50 miles at landfall) the area affected by it was relatively small. As such, a very limited amount of data is available for comparison. The water level response predicted by ACMS at Trident Pier (Figure 14) matches the observed data well, both in terms of the peak water level and phase.

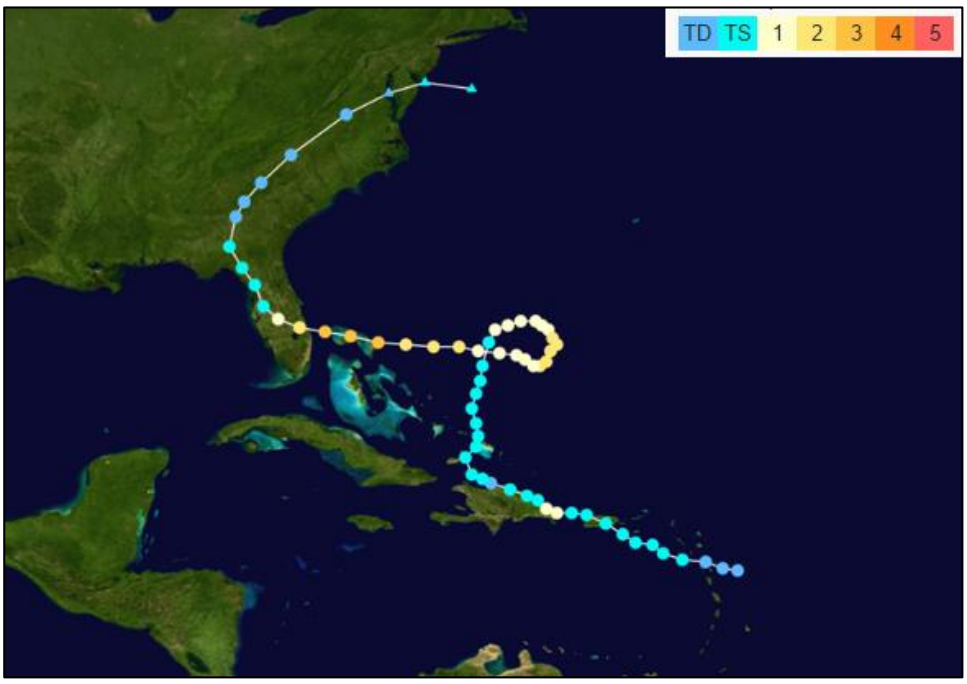

Figure 13. Track of Hurricane Jeanne (2004).

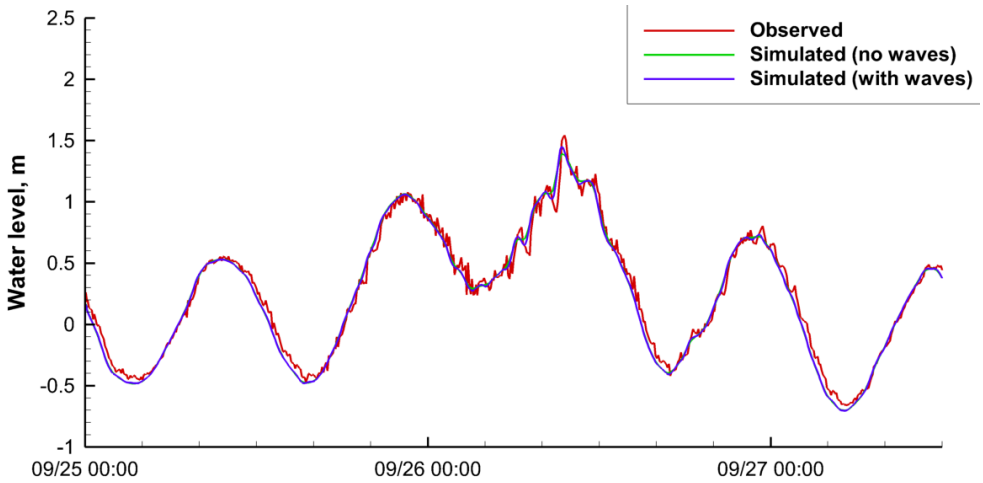

Figure 14. A comparison between simulated (hindcast) and measure waver levels at the Trident Pier Station during Hurricane Jeanne (2004).

Hurricane Wilma (2005)

Hurricane Wilma (Figure 15) was the most intense tropical cyclone ever recorded in the Atlantic basin. In the U.S. it made landfall near Cape Romano, Florida with winds of 120 mph [46] and quickly crossed Florida emerging on the east coast just 5 h later. There is significant amount of data available for Wilma, including over 20 storm gauges that were installed along the west coast of Florida by the USGS. Below is a comparison of peak surge heights at these gauges (Figure 16) and comparison of simulated and observed data at Trident Pier station on the east coast that was affected by the storm after Wilma crossed the Florida peninsula (Figure 17). Maximum storm surge during Wilma was also compared to a number of high water marks and the correlation coefficient between recorded and predicted water marks was 0.78.

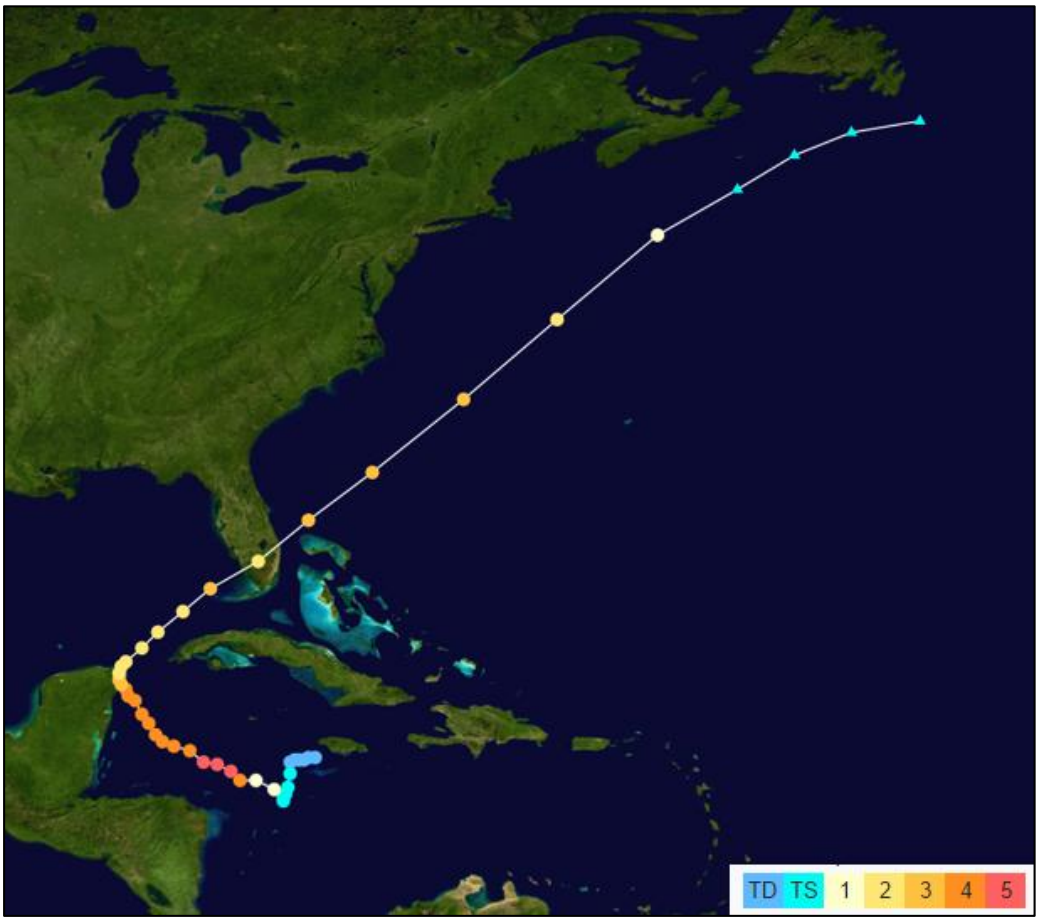

Figure 15. Track of Hurricane Wilma (2005).

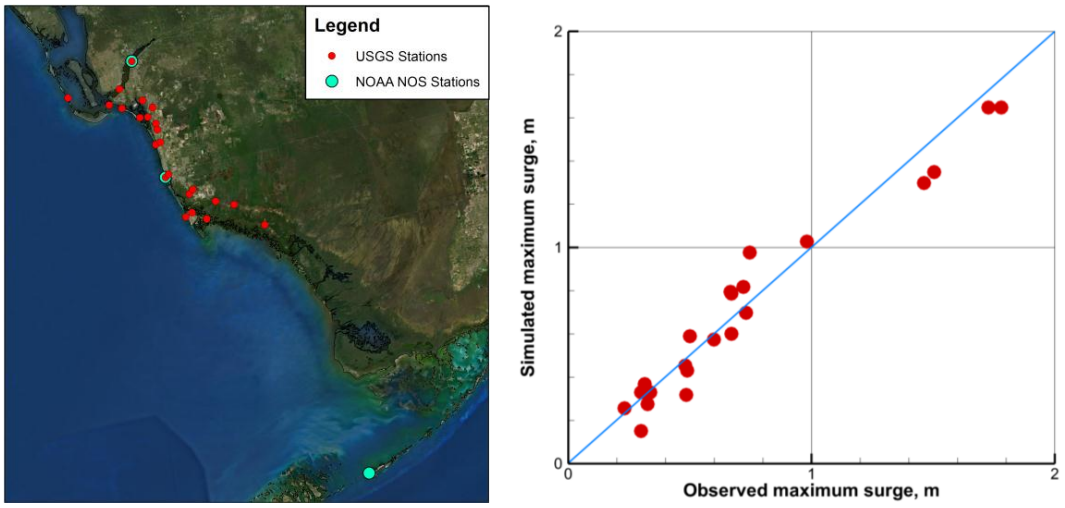

(**a**) (**b**)

Figure 16. Map of data stations with observed data (**a**) and comparison between observed and simulated (hindcast) and peak surges during Hurricane Wilma (**b**).

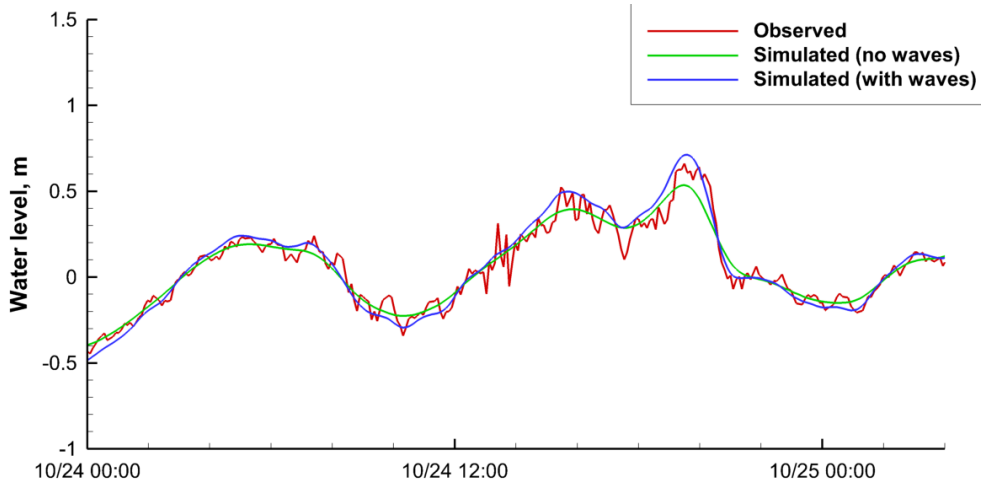

Figure 17. A comparison between simulated (hindcast) and observed water levels at the Trident Pier Station during Hurricane Wilma (2005).

Tropical Storm Fay

The last storm presented for validation purposes is Tropical Storm Fay [47], (Figure 18). It is the weakest storm of the four presented, however, one notable feature of this storm is that it was slowly moving just off the east coast of Florida zigzagging across the coastline over a period of about 24 h making a total of four landfalls in Florida. Fay produced torrential rainfall dropping as much as 27 inches of rain near Melbourne, Florida. The rainfall significantly affected the river flows and salinity making it an interesting case study. Water level comparison at I-295 bridge station (Figure 19) near Jacksonville and salinity comparison at Pine Island station (Figure 20) show that predicted values compare quite well with observed data. It is worth noting that, even though the semidiurnal variations in salinity are only partially captured, the observed significant drop in salinity over the 3-day period was well captured by the model simulation.

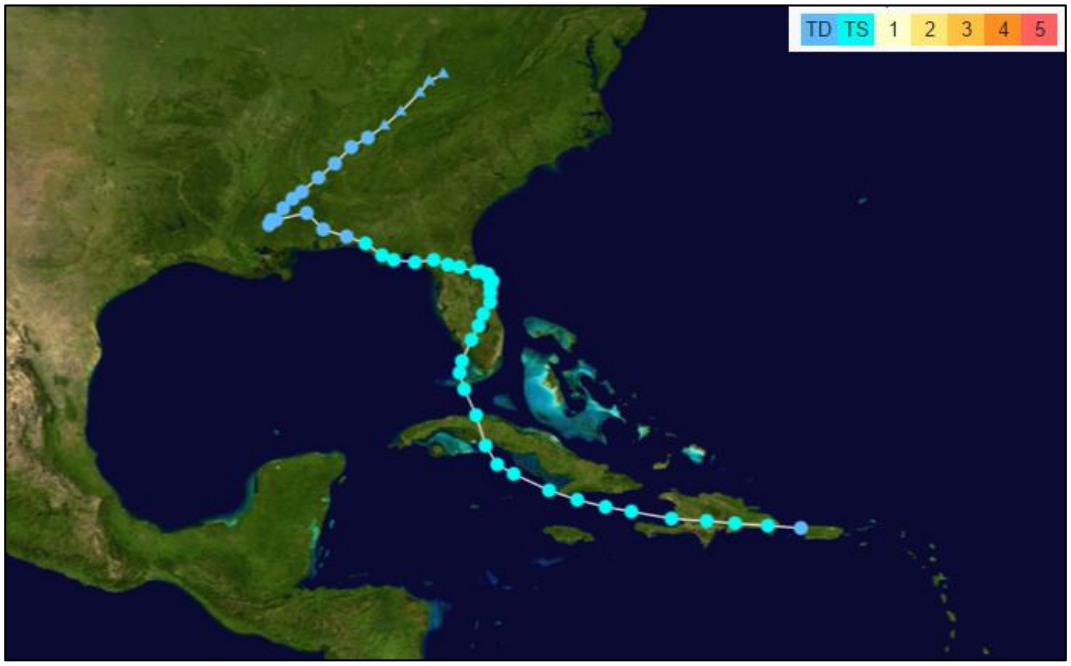

Figure 18. Track of Tropical Cyclone Fay (2008).

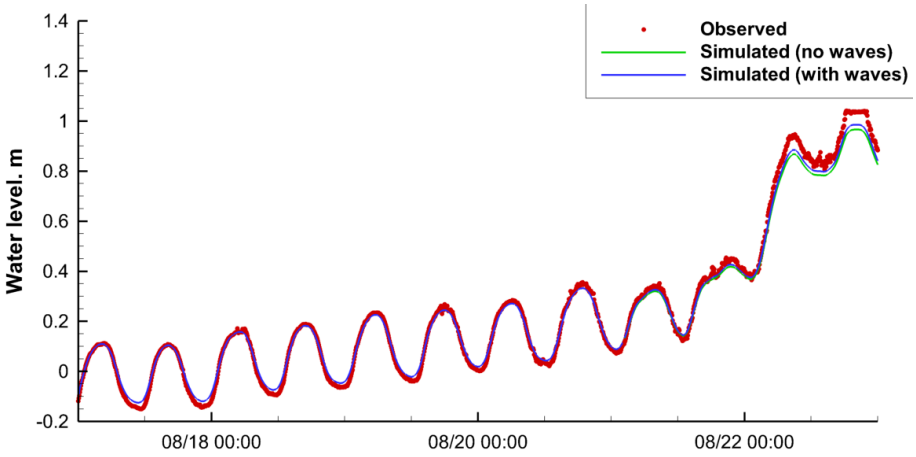

Figure 19. A comparison between the simulated (hindcast) and observed water levels at the I-295 Bridge Station (EC domain) during Tropical Storm Fay (2008).

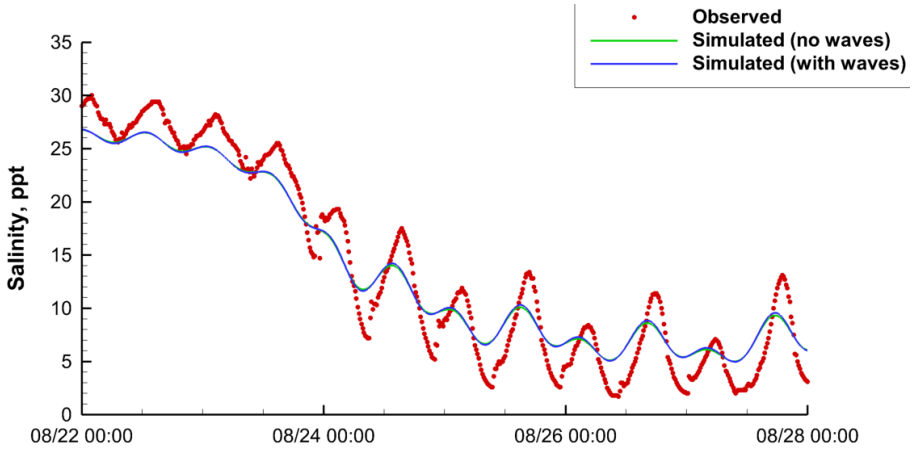

Figure 20. A comparison between simulated (hindcast) and observed salinity at the Pine Island Station (EC domain) during Tropical Cyclone Fay (2008).

3.2. 2015 Hurricane Season Forecasting

ACMS was tested in a quasi-operational mode during the 2015 hurricane season spanning from 1 June 2015 to 30 November 2015. Unfortunately, arrangements for hardware location, networking, etc. are such that it is currently impossible to guarantee a 24/7 uptime for the system as it is located in a research rather than an operational environment and is subject to power and network outages, hardware failures, etc. The system was functioning about 85% of the time. Several statistics were calculated (Table 2) based on these forecasts: root mean square error (RMSE), central frequency (CF), and positive/negative outlier frequency (POF/NOF). These are some of the criteria that are used by NOS for model skill assessment [48]. The error calculations are for the 0–24 h forecast window. Acceptable error limits used for calculation of CF are 15 cm for water level and 3 ppt for salinity and acceptable error limits used for calculation of POF/NOF are 30 cm for water level and 6 ppt for salinity [48].

Table 2. Errors statistics calculated based on ACMS forecasts during 1 June 2015–30 November 2015. Units for root mean square error (RMSE) are cm for water level data and ppt for salinity. Green indicates that the errors are within acceptable limits (>90% for CF and <1% POF/NOF), red indicates otherwise.

Data Station	ACMS Domain	Data Type	Source	RMSE cm/ppt	CF %	POF/NOF %
8728690 Apalachicola	NG	WL	NOAA	7	92.4	0.1/0.3
8727520 Cedar Key	NG	WL	NOAA	6	93.2	0.2/0.3
8726724 Clearwater Beach	SW	WL	NOAA	6	92.0	0.1/0.1
8720219 Dames Point	EC	WL	NOAA	6	93.8	0.2/0.2
8720030 Fernandina Beach	EC	WL	NOAA	5	94.6	0.2/0.1
8725520 Fort Myers	SW	WL	NOAA	4	97.2	0.1/0.0
8720357 I-295 Bridge	EC	WL	NOAA	4	95.6	0.1/0.2
Key West	SE	WL	NOAA	5	95.6	0.1/0.1
Lake Worth Pier	SE	WL	NOAA	6	94.1	0.2/0.2
Mayport	EC	WL	NOAA	4	97.8	0.1/0.0
Mckay Bay	SW	WL	NOAA	5	96.2	0.1/0.1
Naples	SW	WL	NOAA	4	98.2	0.0/0.0
Old Port Tampa	SW	WL	NOAA	5	96.7	0.4/0.2
Panama City	NG	WL	NOAA	5	95.7	0.2/0.7
Pensacola	NG	WL	NOAA	7	93.3	0.4/0.9
Port Manatee	SW	WL	NOAA	6	94.8	0.3/0.2
Racy Point	EC	WL	NOAA	12	86.8	1.4/0.8
Red Bay Point	EC	WL	NOAA	10	91.2	1.1/0.8
S. Riverwalk	EC	WL	NOAA	7	94.0	0.2/0.6
St Petersburg	SW	WL	NOAA	6	94.4	0.3/0.2
Trident Pier	EC	WL	NOAA	5	93.4	0.3/0.3
Vaca Key	SE	WL	NOAA	5	94.8	0.2/0.3
Virginia Key	SE	WL	NOAA	5	96.2	0.2/0.1
Bing's Landing	EC	WL	FLDEP	6	93.2	0.2/0.3
Binney Dock	EC	WL	FLDEP	6	94.7	0.2/0.3
Dry Bar	NG	WL	FLDEP	5	95.3	0.2/0.2
East Bay	NG	WL	FLDEP	6	92.2	0.3/0.6
Gordon River Inlet	SW	WL	FLDEP	5	94.4	0.3/0.1
Melbourne	EC	WL	FLDEP	4	96.6	0.2/0.1
Naples Bay	SW	WL	FLDEP	4	96.3	0.1/0.1
Pilot Cove	NG	WL	FLDEP	7	92.0	0.3/0.5
Ponce de Leon	EC	WL	FLDEP	6	94.5	0.3/0.2
St. Lucie Inlet	EC	WL	FLDEP	5	95.8	0.2/0.2
Tolomato River	EC	WL	FLDEP	7	93.3	0.1/0.3
Vilano Beach	EC	WL	FLDEP	7	94.0	0.1/0.2
Bing's Landing	EC	S	FLDEP	2.1	94.1	0.6/0.4
Dry Bar	NG	S	FLDEP	6.2	77.5	1.7/3.3
Melbourne	EC	S	FLDEP	2.7	88.2	0.7/0.9
Tolomato River	EC	S	FLDEP	1.8	92.9	0.7/0.4
Cat Point	NG	S	ANERR	2.8	87.0	0.8/0.6
Henderson Creek	SW	S	RNERR	1.7	93.7	0.3/0.3
Fakahatchee Bay	SW	S	RNERR	2.3	90.2	0.5/0.4
Faka Union Bay	SW	S	RNERR	2.6	88.2	0.6/0.4
Pellicer Creek	EC	S	GNERR	4.1	81.5	1.5/0.9
San Sebastian	EC	S	GNERR	3.1	86.7	0.8/0.6
Pine Island	EC	S	GNERR	3.3	81.1	1.3/0.8

NOAA—NOAA Tides and Currents [49]; FLDEP—Florida Department of Environmental Protection [50]; ANERR—Apalachicola Bay NERR [51]; RNERR—Rookery Bay NERR [51]; GNERR—Guana-Tolomato-Matanzas NERR [51]; Data types: WL—Water level, S—Salinity.

3.3. Computational Efficiency and Timing

One notable feature of ACMS is its computational efficiency. Currently, model codes run in parallel (implemented via OpenMP) on Intel-based machines running Red Hat Linux (RHEL6/7) with quad-core CPUs (Intel i5-4690 CPU @ 3.50 GHz). Computers are not shared by simulations of different domains or with any other resource-intensive tasks (i.e., each simulation is assigned to a dedicated quad-core machine). The wall times for the full ACMS setup described earlier in this paper for each domain are shown in Table 3.

As noted previously, given the computational efficiency of ACMS provides good balance between the provided accuracy and required resources. In order to run in real time, ACMS needs only 1–4 processing cores, compared to other systems which often require a high-performance computing system with hundreds or thousands of processors. Current ACMS setup uses a single quad-core system (as described above) per model domain. The codes within the system are effectively parallelized and the wall time can be reduced by using more CPU cores. For example, using 32 CPU cores yields approximately 30–40 min wall times (Table 3).

Table 3. Average wall-clock time for ACMS simulations (a simulation consists of a 6-h hindcast/nowcast and a 72-h forecast) per domain. Times can vary from cycle to cycle, depending on conditions and number of wetted grid cells.

Domain	Wall Clock Time (Hours:Minutes)			
	4 CPU Cores		32 CPU Cores	
	2D	3D	2D	3D
East Coast	0:58	3:40	0:22	00:28
Southeast	1:45	5:42	0:37	00:43
Southwest	1:10	4:11	0:29	00:32
Northern Gulf of Mexico	1:29	5:04	0:34	00:37

As such, the 2D and 3D implementations of ACMS differ significantly in wall time required to perform the model simulations, however, this difference only slightly affects the total forecast cycle time. The amount of data required and time needed to fetch these data is significantly different for the 2D and 3D implementations. It can take up to 12 h to obtain all the required boundary conditions for the 3D implementation. The only external data required for the 2D model is a hurricane track as it uses a synthetic parametric wind model to generate wind and pressure fields, which generally takes only minutes to obtain. Pre/post-processing steps take 2–5 min and hence the entire forecast cycle using a 2D model can be completed in less than two hours using the current computational setup.

4. Discussion and Future Work

This paper details how the ACMS was setup, tested, and validated in tidal and hindcast scenarios. The system is shown to be robust and results match well with data for hindcasting. Simulated water levels and salinity for hindcasted periods match well with data and 24-h forecasts that were performed during the 2015 hurricane season are within acceptable limits for most stations. RMS errors for water levels are found to vary between 4 cm and 12 cm. Additional efforts will be undertaken to analyze the sources of error for stations that do not satisfy the criteria (e.g., two stations located upstream the St. Johns River: Racy Point and Red Bay Point) and attempt will be made to reduce the errors. The computational performance of the system is also discussed. Model efficiency allows the production of robust forecasts in a limited-resource environment and choice of NetCDF-based data standards gives flexibility in distributing the data using a THREDDS server and derived products using in-house web-based user interface. The system will be tested in operational settings (completely unattended) and operational performance, uptime, etc. will be a subject of a future publication.

Data availability and its accuracy significantly affect the results of simulations. It is especially important for salinity, as missing river flow or salinity boundary conditions can drastically change the quality of predictions inside an estuary. Additional quality control and data extrapolation methods will be explored along with an option to include a watershed model into ACMS suite for more robust predictions of upstream river flows and subsequently salinity inside estuaries. Temperature is another important variable. While ACMS is capable of simulating temperature, such simulations are currently in the preliminary phase. Feasibility of accurate temperature predictions constrained by limited data is being explored. The key to this is data availability with very little data available for use as boundary

conditions and for validation. Efforts will be made to obtain such data, and setup and validate the temperature model.

Forecasting results from the 2016 hurricane season will be analyzed using more statistical categories and NOS criteria, including maximum duration of positive and negative outliers and worst case outlier frequency, as well as timing of maximums and minimums.

Sheng et al. [52,53] developed a vegetation model which incorporates the effects of vegetation on mean flow and turbulence in the water column. The vegetation resolving model showed that, during hurricanes, total inundation volume can be reduced by up to 40% due to the presence of vegetation. The reduction of storm surge and coastal inundation depends on the characteristics (type, distribution, height, and density, etc.) of vegetation as well as hurricane characteristics (intensity and forward speed, etc.). The vegetation module will be added to the ACMS, however, additional efforts are needed to optimize the algorithms and ensure that this addition does not hinder the efficiency of ACMS.

Acknowledgments: This work was sponsored by the Southeast Coastal Ocean Observing Regional Association (NOAA/NOPP, IOOS.11(033)UF.PS.MOD.1), St. Johns River Water Management District, South Florida Water Management District, and U.S. Fish and Wildlife Service.

Author Contributions: V.A.P., J.R.D. and Y.P.S. conceived and designed model simulation, developed various parts of the model. V.A.P. setup, performed the model simulation, and wrote the paper with Y.P.S.

Conflicts of Interest: The authors declare no conflict of interest. The founding sponsors had no role in the design of the study; in the collection, analyses, or interpretation of data; in the writing of the manuscript, and in the decision to publish the results.

References

1. NOEP (National Ocean Economics Program). Coastal and Ocean Economic Summaries of the Coastal States. 2014. Available online: http://www.oceaneconomics.org/download (accessed on 17 July 2015).
2. NOEP (National Ocean Economics Program). State of the U.S. Ocean and Coastal Economies Coastal States Summaries—2016 Update. 2014. Available online: http://www.oceaneconomics.org/download (accessed on 17 July 2015).
3. NOAA Hurricane Research Division. Detailed List of Continental United States Hurricane Impacts/Landfalls, 1851–1960, 1983–2015. Available online: http://www.aoml.noaa.gov/hrd/hurdat/UShurrs_detailed.html (accessed on 25 August 2016).
4. Jelesnianski, C.P.; Chen, J.; Shaffer, W.A. *SLOSH: Sea, Lake, and Overland Surges from Hurricanes*; US Department of Commerce, National Oceanic and Atmospheric Administration, National Weather Service: Washington, D.C., USA, 1992.
5. Luettich, R.; Westerink, J.J.; Scheffner, N.W. *ADCIRC: An Advanced Three-Dimensional Circulation Model for Shelves Coasts and Estuaries, Report 1: Theory and Methodology of ADCIRC-2DDI and ADCIRC-3DL. DRP-92–6*; U.S. Army Engineers Waterways Experiment Station: Vicksburg, MS, USA, 1992; p. 137.
6. Bleck, R.; Benjamin, S. Regional weather prediction with a model combining terrain following and isentropic coordinates. Part I: Model description. *Mon. Weather Rev.* **1993**, *121*, 1770–1785. [CrossRef]
7. Shchepetkin, A.F.; McWilliams, J.C. The regional oceanic modeling system (ROMS): A split-explicit, free-surface, topography-following-coordinate oceanic model. *Ocean Model.* **2005**, *9*, 347–404. [CrossRef]
8. Barron, C.N.; Kara, A.B.; Hurlburt, H.E.; Rowley, C.; Smedstad, L.F. Sea surface height predictions from the Global Navy Coastal Ocean Model (NCOM) during 1998–2001. *J. Atmos. Ocean. Technol.* **2004**, *21*, 1876–1894. [CrossRef]
9. Sheng, Y.P. *A Three-Dimensional Numerical Model of Coastal and Estuarine Circulation and Transport in Generalized Curvilinear Grids*; Technical Report No. 587; Aeronautical Research Associates Of Princeton: Princeton, NJ, USA, 1986.
10. Sheng, Y.P. *Evolution of a Three-Dimensional Curvilinear-Grid Hydrodynamic Model for Estuaries, Lakes and Coastal Waters: Estuarine and Coastal Modeling I*; ASCE: Reston, VA, USA, 1990; pp. 40–49.
11. Sheng, Y.P.; Paramygin, V.A.; Alymov, V.; Davis, J.R. A Real-Time Forecasting System for Hurricane Induced Storm Surge and Coastal Flooding. In Proceedings of the Ninth International Conference on Estuarine and Coastal Modeling, Charleston, SC, USA, 31 October–2 November 2006; pp. 585–602.

12. Sheng, Y.P.; Alymov, V.; Paramygin, V.A. Simulation of storm surge, waves, and inundation in the Outer Banks and Chesapeake Bay during Hurricane Isabel in 2003: The importance of waves. *J. Geophys. Res.* **2010**, *115*, C4. [CrossRef]
13. Sheng, Y.P.; Zhang, Y.; Paramygin, V.A. Simulation of Storm Surge, Wave, and Coastal Inundation during Hurricane Ivan in 2004. *Ocean Model.* **2010**, *35*, 314–331. [CrossRef]
14. Ris, R.C.; Holthuijsen, L.H.; Booij, N. A third-generation wave model for coastal regions: 2. Verification. *J. Geophys. Res.* **1999**, *104*, 7667–7681. [CrossRef]
15. Sheng, Y.P.; Villaret, C. Modeling the effect of suspended sediment stratification on bottom exchange process. *J. Geophys. Res.* **1989**, *94*, 14429–14444. [CrossRef]
16. Sheng, Y.P.; Kim, T. Skill assessment of an integrated modeling system for shallow coastal and estuarine ecosystems. *J. Mar. Syst.* **2009**, *76*, 212–243. [CrossRef]
17. Sheng, Y.P.; Paramygin, V.A. Forecasting storm surge, inundation, and 3D circulation along the Florida Coast, Estuarine and Coastal Modeling. In Proceedings of the 11th International Conference ASCE, Fort Lauderdale, FL, USA, 20–22 May 2010.
18. Sheng, Y.P.; Paramygin, V.A.; Zhang, Y.; Davis, J.R. Recent enhancements and application of an integrated storm surge modeling system: CH3D-SSMS. Estuarine and Coastal Modeling. In Proceedings of the Tenth International Conference ASCE, New Orleans, LA, USA, 9–12 March 2008; pp. 879–892.
19. Sheng, Y.P.; Tutak, B.; Davis, J.R.; Paramygin, V. Circulation and flushing in the lagoonal system of the Guana Tolomato Matanzas National Estuarine Research Reserve (GTMNERR), Florida. *J. Coast. Res.* **2008**, *55*, 9–25. [CrossRef]
20. Davis, J.R.; Sheng, Y.P. Development of a parallel storm surge model. *Int. J. Numer. Meth. Fluids* **2003**, *42*, 549–580. [CrossRef]
21. Sheng, Y.P.; Davis, J.R.; Figueiredo, R.; Liu, B.; Liu, H.; Luettich, R., Jr.; Paramygin, V.A.; Weaver, R.; Weisberg, R.; Xie, L.; et al. A Regional Testbed for Storm Surge and Inundation Models. In Proceedings of the 12th International Conference on Estuarine and Coastal Modeling, St. Augustine, FL, USA, 7–9 November 2011.
22. Peng, M.; Xie, L.; Pietrafesa, L.J. A numerical study of storm surge and inundation in the Croatan–Albemarle–Pamlico Estuary System. *Estuar. Coast. Shelf Sci.* **2004**, *59*, 121–137. [CrossRef]
23. Chen, C.; Cowles, G.; Beardsley, R.C. *An Unstructured Grid, Finite Volume Coastal Ocean Model: FVCOM User Manual*, 2nd ed.; SMAST/UMASSD TR-06–0602; MIT: Cambridge, MA, USA, 2006; p. 315.
24. National Academy of Sciences. *Mapping the Zone—Improving Flood Map Accuracy*; Committee on FEMA Flood Maps, National Research Council: Washington, DC, USA, 2009.
25. Lapetina, A.; Sheng, Y.P. Simulating complex storm surge dynamics: Three-dimensionality, vegetation effect, and onshore sediment transport. *J. Geophys. Res. Oceans* **2015**, *120*, 7363–7380. [CrossRef]
26. Powell, M.D.; Houston, S.H.; Amat, L.R.; Morisseau-Leroy, N. The HRD real-time hurricane wind analysis system. *J. Wind Eng. Ind. Aerodyn.* **1998**, *77*, 53–64. [CrossRef]
27. NOGAPS. Available online: http://coaps.fsu.edu/woce/html/models/fnoc.htm (accessed on 8 January 2017).
28. About the GFDL Hurricane Model Ensemble. Available online: http://data1.gfdl.noaa.gov/hurricane/gfdl_ensemble/about.html (accessed on 8 January 2017).
29. Michalakes, J.; Dudhia, J.; Gill, D.; Henderson, T.; Klemp, J.; Skamarock, W.; Wang, W. The Weather Reseach and Forecast Model: Software Architecture and Performance. In Proceedings of the 11th ECMWF Workshop on the Use of High Performance Computing In Meteorology, Reading, UK, 25–29 October 2004.
30. NAM Products. Available online: http://www.nco.ncep.noaa.gov/pmb/products/nam (accessed on 8 January 2017).
31. Davis, J.R.; Paramygin, V.A.; Forrest, D.; Sheng, Y.P. Towards the probabilistic simulation of storm surge and inundation in a limited resource environment. *Mon. Weather Rev.* **2010**, *138*, 2953–2974. [CrossRef]
32. Miller, R.J.; Schrader, A.J.; Sampson, C.R.; Tsui, T.L. The Automated Tropical Cyclone Forecasting System (ATCF). *Weather Forecast.* **1990**, *5*, 653–660. [CrossRef]
33. Halliwell, G. Evaluation of vertical coordinate and vertical mixing algorithms in the HYbrid Coordinate Ocean Model (HYCOM). *Ocean Modelling.* **2004**, *7*, 285–322. [CrossRef]
34. Tolman, H.L. *User Manual and System Documentation of WAVEWATCH III Version 3.14. NOAA/NWS/NCEP/MMAB Technical Note 276*; National Weather Service: Camp Springs, MD, USA, 2009; p. 194.
35. HTCondor—Home. Available online: https://research.cs.wisc.edu/htcondor (accessed on 1 July 2016).

36. THREDDS Data Server. Available online: http://www.unidata.ucar.edu/software/thredds/current/tds (accessed on 15 June 2016).
37. Xie, L.; Bao, S.; Pietrafesa, L.J.; Foley, K.; Fuentes, M. A Real-Time Hurricane Surface Wind Forecasting Model: Formulation and Verification. *Mon. Weather Rev.* **2006**, *134*, 1355–1370. [CrossRef]
38. Sheng, Y.P.; Liu, T. Three-dimensional simulation of wave-induced circulation: Comparison of three radiation stress formulations. *J. Geophys. Res.* **2011**, *116*, C05021. [CrossRef]
39. Mellor, G.L. The depth dependent current and wave interaction equations: A revision. *J. Phys. Oceangr.* **2008**, *38*, 2587–2596. [CrossRef]
40. Longuet-Higgins, M.S.; Stewart, R.W. Radiation stress and mass transport in gravity waves with application to 'surf beats'. *J. Fluid Mech.* **1962**, *13*, 481–504. [CrossRef]
41. Longuet-Higgins, M.S.; Stewart, R.W. Radiation stresses in water waves: A physical discussion with applications. *Deep-Sea Res.* **1964**, *11*, 529–562. [CrossRef]
42. Parks, A.B.; Shay, L.K.; Johns, W.E.; Martinez-Pedraja, J.; Gurgel, K.-W. HF radar observations of small-scale surface current variability in the Straits of Florida. *J. Geophys. Res.* **2009**, *114*, C08002. [CrossRef]
43. Shay, L.K.; Cook, T.M.; Peters, H.; Mariano, A.J.; Weisberg, R.; An, P.E.; Soloviev, A.; Luther, M. Very High Frequency Radar Mapping of Surface Currents. *IEEE J. Coast. Eng.* **2002**, *27*, 155–169. [CrossRef]
44. Landsea, C.W.; Franklin, J.L.; McAdie, C.J.; Beven, J.L., II; Gross, J.M.; Jarvinen, B.R.; Pasch, R.J.; Rappaport, E.N.; Dunion, J.P.; Dodge, P.P. A reanalysis of hurricane Andrew's intensity. *Am. Meteorol. Soc.* **2004**, *85*, 1699. [CrossRef]
45. Lawrence, M.B.; Cobb, H.D. *Tropical Cyclone Report Hurricane Jeanne 13–28 September 2004*; National Hurricane Center: Miami, FL, USA, 2005.
46. Pasch, R.J.; Blake, E.S.; Cobb, H.D., III; Roberts, D.P. *Tropical Cyclone Report Hurricane Wilma. 15–25 October 2005*; National Hurricane Center: Miami, FL, USA, 2006.
47. Stewart, S.R.; Beven, J.L., II. *Tropical Cyclone Report Tropical Cyclone Fay (AL062008) 15–26 August 2008*; National Hurricane Center: Miami, FL, USA, 2009.
48. Kelley, J.G.W.; Zhang, A.; Chu, P.; Lang, G.A. *Skill Assessment of NOS Lake Huron Operational Forecast System (LHOFS)*; NOAA Technical Memorandum NOS CS 23: Silver Spring, MD, USA, 2010.
49. NOAA Tides and Currents. Available online: https://tidesandcurrents.noaa.gov (accessed on 8 January 2017).
50. Florida Department of Environmental Protection/Division of State Lands/Bureau of Survey and Mapping. Available online: http://www.fldep-stevens.com (accessed on 8 January 2017).
51. Centralized Data Management Office. Available online: http://cdmo.baruch.sc.edu/get/landing.cfm (accessed on 8 January 2017).
52. Sheng, Y.P.; Lapetina, A.; Ma, G. The reduction of storm surge by vegetation canopies: Three-dimensional simulations. *Geophys. Res. Lett.* **2012**, *39*, L20601. [CrossRef]
53. Lapetina, A.; Sheng, Y.P. Three-dimensional modeling of storm surge and inundation including the effects of coastal vegetation. *Estuaries Coasts* **2014**. [CrossRef]